Novel mode of antagonist binding in NMDA receptors revealed by the crystal structure of the GluN1-GluN2A ligand-binding domain complexed to NVP-AAM077

Annabel Romero-Hernandez and Hiro Furukawa

Keck Structural Biology Laboratory, Cold Spring Harbor Laboratory, Cold Spring Harbor, NY, 11724, USA (AR-H and HF)

Watson School of Biological Sciences, Cold Spring Harbor, NY, 11724, USA (AR-H and HF)

a) **Running Title:** Crystal structure of NMDA receptor bound to NVP-AAM077

b) **Contact (Corresponding Author)**

Hiro Furukawa

One Bungtown Rd., Cold Spring Harbor, NY, 11724, USA

Email: furukawa@cshl.edu

TEL: 516-367-8872

c) **Manuscript Info**

Text Pages: 28

Figure 1-6

Table 1-2

References: 34

Number of words in the -

Abstract: 167

Introduction: 720

Discussion: 748

d) **Non-Standard Abbreviations:** NMDA, *N*-methyl-D-aspartate; NVP-AAM077, (R)-[(S)-1-(4-bromo-phenyl)-ethylamino]-(2,3-dioxo-1,2,3,4-tetrahydroquinoxalin-5-yl)-methyl]-phosphonic acid; PPDA, 1-(phenanthrene-2-carbonyl)-piperazine-2, 3-dicarboxylic acid; D-AP5, D-(-)-2-Amino-5-phosphonopentanoic acid; DCKA, 5,7-dichlorokynurenic acid; iGluRs, ionotropic glutamate receptors; AMPA, α-amino-3-hydroxy-5-methyl-4-isoxazole propionic acid ; ATD, amino terminal domain; LBD, ligand-binding domain; TMD, transmembrane domain; CTD, carboxyl-terminal domain;

Abstract

Competitive antagonists against *N*-methyl-D-aspartate (NMDA) receptors have played critical roles throughout the history of neuropharmacology and basic neuroscience. There are currently numerous NMDA receptor antagonists containing a variety of chemical groups. Among those compounds, a GluN2-specific antagonist, (R)-[(S)-1-(4-bromo-phenyl)-ethylamino]-(2,3-dioxo-1,2,3,4-tetrahydroquinoxalin-5-yl)-methyl]-phosphonic acid (NVP-AAM077), contains a unique combination of a dioxoquinoxalinyl ring, a bromophenyl group, and a phosphono group. Here, we present the crystal structure of the isolated ligand-binding domain (LBD) of the GluN1-GluN2A NMDA receptor in complex with the GluN1 agonist glycine and the GluN2A antagonist NVP-AAM077. The structure shows placement of the dioxoquinoxalinyl ring and the phosphono group of NVP-AAM077 in the glutamate binding pocket in GluN2A and the novel interaction between the bromophenyl group and GluN1-Glu781 at the GluN1-GluN2A subunit interface. Site-directed mutagenesis of GluN1-Glu781 reduced the potency of inhibition by NVP-AAM077, thus confirming the involvement of the GluN1 subunit for binding of NVP-AAM077. The unique antagonist binding pattern shown in this study provides a novel dimension to design and create antagonists with potential therapeutic values.

Introduction

Antagonists against NMDA receptors have played critical roles to delineate the physiological roles of NMDA receptors in brain functions and in neurological disorders and diseases in many studies. NMDA receptors belong to the large family of ionotropic glutamate receptors (iGluRs) that mediate the majority of fast excitatory synaptic transmission in the mammalian brain. Dysfunctional NMDA receptors have been implicated in various neurological disorders and diseases including schizophrenia, depression, Alzheimer's disease, stroke, and seizure. Thus, in addition to applications in basic neuroscience research, NMDA receptor antagonists have drawn significant attention as potential therapeutic reagents. The effort to develop competitive NMDA receptor antagonists started from D-α-aminoadipate (DαAA) (McLennan and Lodge, 1979) with moderate specificity and potency leading to the significantly more potent NMDA-selective compound, D-(-)-2-Amino-5-phosphonopentanoic acid (D-AP5) (Evans et al., 1982) containing the amino acid backbone and a phosphono group. This was followed by compounds with phenanthrene backbones such as 1-(phenanthrene-2-carbonyl)-piperazine-2, 3-dicarboxylic acid (PPDA) (Feng et al., 2004). Furthermore, another compound, (R)-[(S)-1-(4-bromo-phenyl)-ethylamino]-(2,3-dioxo-1,2,3,4-tetrahydroquinoxalin-5-yl)-methyl]-phosphonic acid (NVP-AAM077), with an anticonvulsant effect in animals became available (Auberson et al., 2002) (Fig. 1A). NVP-AAM077 was originally reported to have over 100-fold specificity towards the GluN1-GluN2A NMDA receptors over GluN1-GluN2B NMDA receptors but was later shown to have only ~5-fold specificity through more accurate and extensive pharmacological analyses (Frizelle et al., 2006).

NMDA receptors, like any other iGluR family members, are heterotetrameric ion channels composed of two GluN1 subunits and two GluN2 and/or GluN3 subunits (Traynelis et al., 2010). The eight splice variants of the GluN1 subunits (1a-4a and 1b-4b) and the two GluN3 subunits (A-B) bind to glycine whereas the four GluN2 subunits (A-D) bind to glutamate or NMDA. All of the above subunits contain modular domains including an amino-terminal domain (ATD), a ligand-binding domain (LBD), a transmembrane domain (TMD), and a carboxyl-terminal domain (CTD) (Fig. 1B). The LBDs bind agonists, co-agonists, competitive antagonists, and allosteric modulators to control gating properties of the ion channel pore formed by the TMD. The ATD regulates channel properties such as open probability and speeds of activation and deactivation (Gielen et al., 2009; Yuan et al., 2009), and also binds to allosteric modulators to either potentiate or inhibit the channel activities (Karakas et al., 2011; Williams, 1993, 1997) in a subtype-specific manner.

Our recent crystallographic study on the GluN1-GluN2A LBD unraveled the binding pattern of two antagonists, D-AP5 and PPDA (Jespersen et al., 2014). This study showed that the alpha-carboxylate group contained in both of these compounds interacts with a conserved arginine residue (Arg518 in GluN2A) while distinct chemical moieties of D-AP5 and PPDA occupy different sub-sites, which we named Site-I and Site-II (Jespersen et al., 2014). Specifically, Site-I accommodates the phosphono-group of D-AP5 via direct polar interactions and Site-II binds to the phenanthrene group of PPDA mainly via hydrophobic interactions. A compound that does not occupy Site-I, such as PPDA, can also bind and inhibit α-amino-3-hydroxy-5-methyl-4-isoxazole propionic acid (AMPA) receptors and kainate receptors indicating that the interaction

between Site-I and the phosphono-group is a critical determinant for the specificity towards NMDA receptors. NVP-AAM077 has a unique bromophenyl substitution at the amino group nitrogen, which led us to hypothesize that the binding mode for NVP-AAM077 may be distinct from the ones for D-AP5 and PPDA. Structural studies on the intact NMDA receptor ion channels by x-ray crystallography and cryo-electron microscopy have shown patterns of conformational alterations linked to functions in multiple domains, which are associated with activation and inhibition (Karakas and Furukawa, 2014; Lee et al., 2014; Tajima et al., 2016; Zhu et al., 2016). However, the structural studies on the intact NMDA receptors have not been ideal for monitoring exact compound binding modes at the atomic level due to their low resolution nature (3.6 to 15 Å). For this reason, in this study, we implemented x-ray crystallography on the isolated GluN1-GluN2A LBD heterodimer, which is amenable to high-resolution structural analysis. We report here a crystal structure of the GluN1-GluN2A LBD complexed to NVP-AAM077 at 1.6 Å resolution. The structure shows a previously unobserved mode of antagonist-binding involving residues from both GluN1 and GluN2A. Despite the unique binding mode, the NVP-AAM077 binding stabilizes the open-cleft conformation of the bi-lobed architecture of the GluN2A LBD in a similar manner to the D-AP5 and PPDA bindings. Additionally, the crystal structure also explains why NVP-AAM077 does not qualify as a GluN2A-specific antagonist.

Materials and Methods

Expression and purification of GluN1 and GluN2A LBDs

The rat GluN1 LBD is defined as S1 (Met394 to Lys544) and S2 (Arg663 to Ser800) connected by a Gly-Thr linker and was expressed in OrigamiB (DE3) cells (Novagen) under the T7 promoter in pET22b(+) as described previously (Furukawa and Gouaux, 2003; Jespersen et al., 2014). After growing cells to an OD_{600} = 1.5, protein expression was induced by 0.5 mM isopropyl-beta-D-1-thiogalactopyranoside (IPTG) for 22 hrs. at 15°C. The protein was purified using Nickel-Nitrilotriacetic acid (NTA) Chelating Sepharose followed by thrombin digestion to remove the polyhistidine tag. The digested product was purified by an SP-Sepharose column (GE Healthcare). The rat GluN2A LBD composed of S1 (Asp402 to Arg539) and S2 (Gln661 to Asn802) connected by a Gly-Thr dipeptide linker was expressed as a fusion protein to small ubiquitin-like modifier (SUMO) with a hexa-histidine tag at the N terminus in OrigamiB (DE3) cells in the same way as for GluN1 LBD. Protein purification was conducted using Nickel-NTA Chelating Sepharose chromatography, followed by digestion by ubiquitin ligase protease-1 to remove SUMO. The digested product was further purified by Q-Sepharose and SP-Sepharose ion exchange chromatography (GE Healthcare) as described previously (Jespersen et al., 2014).

Crystallography

Purified GluN1 and GluN2A LBD proteins were individually concentrated to 6 mg/ml, mixed at a 1:1 (w/w) ratio and dialyzed against a buffer containing 10 mM HEPES-NaOH (pH 7.0), 100 mM NaCl, 1 mM L-glutamate and 10 µM glycine at 4°C overnight. The GluN1-GluN2A LBD crystals were produced by vapor diffusion at 18°C by the hanging drop method. Specifically, the purified proteins and the reservoir solution

containing 18% polyethylene glycol monomethylether 2000 (PEG2000 MME), 100 mM

HEPES-NaOH (pH 7.0), and 75 mM NaCl were mixed at a 2:1 volume ratio and vapor

diffused against the reservoir solution. Crystals appeared after one to two days. Crystals

were then soaked against a buffer (100 mM HEPES pH 7.0, 75 mM NaCl, 18% PEG

2000 MME and 1 mM glycine) supplemented with 0.2 mM NVP-AAM077 for 12 hrs. and

with 0.4 mM NVP-AAM077 for another 5 hrs. Finally, crystals were soaked against a

buffer containing 1 mM NVP-AAM077 and 18% glycerol for a few seconds and

immediately flash frozen by liquid nitrogen. X-ray diffraction data was collect at X29 at

the National Synchrotron Light Source at Brookhaven National Laboratory and

processed using HKL2000 (Otwinowski and Minor, 1997). All of the structures were

determined by molecular replacement using three search probes: GluN1 LBD, GluN2A

LBD Domain 1 (Asn404-Glu530 and Gly760-His801), and GluN2A LBD Domain 2

(Thr531-Thr759) from the structural coordinate of the GluN1-GluN2A LBD (PDB code:

4NF8) (Jespersen et al., 2014). Rotational and translational search by the program

PHASER (McCoy et al., 2007) resulted in the Z scores and LLG values were RFZ= 20.7,

TFZ= 28.0, and LLG= 869 for GluN1 LBD, RFZ= 13, TFZ= 44.7, and LLG= 2345 for

GluN2A LBD Domain 2, and RFZ= 11.9, TFZ= 51.5, and LLG= 4204, for GluN2A LBD

Domain 2. Structural refinement and model building were performed with PHENIX

(Adams et al., 2002) and Coot (Emsley and Cowtan, 2004), respectively. The degree of

domain opening between the glutamate-bound GluN2A LBD and the NVP-AAM077-

bound GluN2A LBD was calculated using the program Pymol and running the python

script, draw_rotation_axis.py (code written by Pablo Guardado Calvo downloaded from

the pymolwiki website). Specifically, the Cαs of the D1 regions were first superimposed

by the 'super' command in Pymol. The transformation matrix to superpose the Cαs of the D2 regions was calculated and used to generate a rotation axis.

Electrophysiology

Recombinant GluN1-1a/GluN2A NMDA receptors were expressed by co-injecting 0.1–0.5 ng of the wild-type or mutant rat GluN1-1a and GluN2A cRNAs at a 1:1 ratio (w/w) into defolliculated *Xenopus laevis* oocytes. The two-electrode voltage-clamp (TEVC) recordings were performed using agarose-tipped microelectrodes (0.4–1.0 MΩ) filled with 3 M KCl at a holding potential of -60 mV. The bath solution contained 5 mM HEPES, 100 mM NaCl, 0.3 mM $BaCl_2$, at pH 7.4 (adjusted with potassium hydroxide [KOH]). Currents were evoked by applications of 100 µM of glycine and various concentrations of L-glutamate. For analyzing inhibition by NVP-AAM077, various concentrations of antagonists were applied in the presence of 5 µM L-glutamate. The data sets were acquired and analyzed by the program Pulse (HEKA). Data points were plotted and fitted to calculate EC_{50} values of L-glutamate and IC_{50} values of antagonists using the program Kaleidagraph (Synergy Software). K_i values were calculated with the Cheng-Prusoff equation: $K_i = IC_{50}/(1 + [\text{L-glutamate}]/EC_{50})$.

Results

Structural study of GluN1-GluN2A LBD complexed to NVP-AAM077

To understand the binding mode and the resulting effect on the overall protein conformation, we attempted to obtain the high-resolution structure of the isolated LBD proteins. Towards this end, we took advantage of our previously established method for effectively obtaining high-resolution structures of the GluN1-GluN2A LBD complexed to antagonists (Jespersen et al., 2014). Specifically, the crystals of the GluN1-GluN2A LBD proteins were grown in the presence of glycine and glutamate, and soaked against the crystallization buffer (see Materials and Methods) containing glycine and NVP-AAM077. Thus, in the crystal structure the co-agonist glycine is bound to the GluN1 LBD and the antagonist NVP-AAM077 is bound to the GluN2A LBD. Our crystals gave rise to x-ray diffraction to the Bragg spacing of 1.6 Å (Table 1). The electron density was visible for 283 residues out of the 289 residues derived from GluN1 and all of the 280 residues derived from GluN2A. The quality of the electron density was especially high at the GluN1-GluN2A subunit interface and at the NVP-AAM077 binding site, which allowed us to monitor the precise binding mode of NVP-AAM077 and the hydrogen bond network around the binding site.

Overall architecture of NVP-AAM077-GluN1-GluN2A LBD

Both the GluN1 and GluN2A LBDs have the bi-lobed clamshell-like architecture composed of an upper domain (D1) and a lower domain (D2) as previously observed (Fig. 1 and 2) (Furukawa and Gouaux, 2003; Furukawa et al., 2005; Jespersen et al., 2014). The GluN1 and GluN2A LBD proteins crystallized as a heterodimer as in the previous case (Jespersen et al., 2014). This heterodimeric subunit arrangement is

physiological as the similar GluN1-GluN2A LBD heterodimer is observed in the structure of the intact heterotetrameric NMDA receptor ion channels (Karakas and Furukawa, 2014; Lee et al., 2014). The main locus for the NVP-AAM077 binding is the D1-D2 domain cleft in the GluN2A subunit where the neurotransmitter agonist, glutamate, also binds. Furthermore, the bromophenyl group of NVP-AAM077 extends toward the GluN1 subunit (Fig. 2B) and makes an additional contact with a GluN1 residue as described in more detail in the following sections.

Comparison with GluN1-GluN2A LBD bound to glutamate and other antagonists

Binding of NVP-AAM077 to the GluN1-GluN2A LBD results in the rigid-body 'opening' of the D1-D2 bi-lobe in GluN2A compared to that bound to glutamate (Fig. 3). Stabilization of the open conformation upon binding of competitive antagonists is a feature previously observed in the structural studies of the GluN1-GluN2A LBD complexed to D-AP5 and (-)-PPDA (Jespersen et al., 2014). The degree of the bi-lobe opening is ~16°, ~21°, and ~17° for D-AP5, PPDA, and NVP-AAM077, respectively (Fig. 3B, Materials and Methods). Thus, the extent of bi-lobe opening in the NVP-AAM077-bound GluN2A LBD is more similar to that of the D-AP5-bound GluN2A LBD than the PPDA-bound GluN2A LBD.

The opening and closing motions of the LBD bi-lobes are considered important for controlling ion channel gating in iGluRs. In NMDA receptors, the closure of the bi-lobes by agonist binding is suggested to move the LBD-TMD linkers of the GluN1 and GluN2A subunits apart to create a tension that is required to move the pore forming M3

11

transmembrane helices (Kazi et al., 2014). Contrary to agonist binding, antagonist binding stabilizes the LBD bi-lobes in an open conformation thereby keeping the distance between the LBD-TMD linkers of GluN1 and GluN2A sufficiently short. This prevents formation of tensions, thus, the TMD ion channels remain closed (Fig. 3). The residues GluN1-Ile664 and GluN2A-Val662 are located at the upper edge of the LBD-TMD linker and are subject to movement upon ligand binding (Fig. 3C). Upon binding of NVP-AAM077 to GluN2A, the distance between GluN1-Ile664 and GluN2A-Val662 shortens by 3.9 Å compared to that when glutamate is bound. Contrary to the GluN2A LBD, there is little or no change in the GluN1 subunit between the glutamate-bound and NVP-AAM077-bound GluN1-GluN2A LBD as represented by the low root-mean-square deviation distance (RMSD) (0.53 Å over 275 Cα positions). No apparent change was observed in the pattern of the GluN1-GluN2A subunit arrangement.

Novel binding mode of NVP-AAM077

The 1.6 Å resolution structure from the current crystallographic study provided an accurate map of the compound binding site (Fig. 4 and Table 1). Substitution of glutamate with NVP-AAM077 was near complete as there is no visual evidence for the remaining glutamate density after extensive crystal soaking. Our previous studies revealed elements of the binding pocket important for recognition of D-AP5 and PPDA (Jespersen et al., 2014). The phosphono group in D-AP5 occupies the subsite, Site-I, consisting of polar residues including GluN2A-Ser689, GluN2A-Thr690, and GluN2A-Tyr730 whereas the phenanthrene group in PPDA occupies the subsite, Site-II,

consisting of hydrophobic residues (Jespersen et al., 2014). Binding of NVP-AAM077 is mediated by a number of direct interactions including polar interactions between the dioxoquinoxalinyl group and residues from D1 (GluN2A-Ser511, -Thr513, and -Arg518), the phosphono group and residues from Site-I, and the bromophenyl group and GluN1-Glu781 at Site-III (Fig. 4C). The extension of the bromophenyl group towards the GluN1-GluN2A subunit interface and the direct interaction of the bromine atom with the carboxylate group of GluN1-Glu781 at Site-III is a binding mode previously unobserved. The placement of the bromophenyl group at Site-III displaces three water molecules present in the glutamate-GluN1-GluN2A LBD, which are involved in water-mediated polar interactions that tethers GluN1-Glu781 and GluN2A-Ser689 or GluN2A-Thr690, thereby stabilizing the inter-subunit interaction in addition to the 'opening' the GluN2A bi-lobe (Fig. 5). The distance between the bromine atom from NVP-AAM077 and the carboxylate group of GluN1-Glu781 is 3.5 Å, which slightly deviates from the ideal distance for bond formation (suggested to be 3.37 Å for a bromine-oxygen interaction) (Auffinger et al., 2004; Sirimulla et al., 2013). We speculate that a weak bromine-oxygen interaction exists between GluN1-Glu781 and a bromine atom because the electron density for the bromophenyl group and the GluN1-Glu781 is highly ordered (Fig. 5A and B). Other key interactions between NVP-AAM077 and the GluN1-GluN2A LBD include polar interactions between the dioxoquinoline group and GluN2A-Ser689, the amino-bromophenyl group and GluN2A-Thr690, and water-mediated hydrogen bonds involving GluN2A-Val685, -Pro686, -Gly688, and -Glu691 (W1 and W2; Fig. 4A).

Validation of NVP-AAM077 binding mode

To validate the physiological relevance of the new antagonist binding mode observed in the NVP-AAM077-GluN1-GluN2A LBD structure, we conducted site-directed mutagenesis coupled with two-electrode voltage clamp (TEVC). While the binding pattern in Site-I is similar between the NVP-AAM077- and D-AP5-bound structures, the compound recognition by Site-III at the GluN1-GluN2A LBD interface is unprecedented (Fig. 4 and 5). Thus, we focused on validating the importance of Site-III by conducting site-directed mutagenesis of GluN1-Glu781, which interacts with the bromine atom in the bromophenyl group of NVP-AAM077. We mutated GluN1-Glu781 to aspartate or alanine to alter the distance between the carboxylate group and the bromine atom or to remove the carboxylate group, respectively. We estimated K_i values by measuring the EC_{50} of glutamate and IC_{50} of NVP-AAM077 (Fig. 6 and Supplemental Fig. 1). As predicted by the presence of the water-mediated hydrogen bond network in Site-III in the glutamate-GluN1-GluN2A LBD structure (Fig. 5C), we saw changes in the glutamate potency when this network was broken by the GluN1-Glu781Asp and the GluN1-Glu781Ala mutations indicating the importance of the subunit interface in activity (Fig. 6A). Nevertheless, the K_i values for NVP-AAM077 in the GluN1-Glu781Asp and -Glu781Ala mutants were greater by ~13-fold and 9-fold compared to the wildtype, respectively (Fig. 6B and C, Table 2). Thus, the mutagenesis result indicated that the interaction between the bromophenyl group in NVP-AAM077 and GluN1-Glu781 is critical for inhibition.

Discussion

14

The current high-resolution structural study revealed a novel antagonist-binding mode of NVP-AAM077. Specifically, the bromophenyl group of NVP-AAM077 extends out of the glutamate binding pocket in GluN2A towards the GluN1-GluN2A subunit interface, and interacts with GluN1-Glu781. This marks the first example where a competitive antagonist for NMDA receptors is recognized by residues from both GluN1 and GluN2 subunits.

The subunit interfaces in iGluRs are generally known to be critical for regulating activities of their oligomeric ion channels (Karakas et al., 2015; Regan et al., 2015). Some of the subunit interfaces in iGluRs also serve as binding sites for compounds for functional regulation. Such an example in NMDA receptors is an allosteric inhibitor, ifenprodil, which binds to the GluN1-GluN2B subunit interface at ATD (Karakas et al., 2011). Other examples are binding of negative allosteric modulator (NAM) and positive allosteric modulator (PAM) compounds, which have been shown to occur at the GluN1-GluN2A LBD subunit interface by recent structural studies (Hackos et al., 2016; Yi et al., 2016). Even though the molecular mechanism is yet to be determined clearly, these studies indicated that stabilization of the subunit interface can up-regulate or down-regulate the ion channel activity. In AMPA receptors, the subunit interface of the LBD homodimer accommodates cyclothiazide (CTZ) and aniracetam, which alleviate desensitization and slow the speed of deactivation (Jin et al., 2005; Sun et al., 2002). The stabilization of the subunit interface by a mutation or artificial disulfide cross-link in AMPA receptors has also been shown to reduce desensitization indicating that the strength of the inter-subunit interaction in AMPA receptors controls the ion channel function (Stern-Bach et al., 1998; Weston et al., 2006). Of note is the fact that there is

no positional overlap between binding sites of NVP-AAM077 and the NMDA receptor NAMs, thus, the inhibitory effect of NVP-AAM077 is likely distinct from that of NAM even though a portion of NVP-AAM077 resides at the subunit interface.

Binding of NVP-AAM077 results in 'opening' of the bi-lobe of the GluN2A LBD compared to the glutamate-bound GluN2A LBD. A similar pattern of rigid body domain movement was previously observed in the GluN1-GluN2A LBD bound to D-AP5 and PPDA (Jespersen et al., 2014). The recent structural study on the intact GluN1-GluN2B NMDA receptors solved in the presence of antagonists for both GluN1 and GluN2 subunits, 5,7-dichlorokynurenic acid (DCKA) and D-AP5, showed extensive disruption of the LBD subunit interface where NAM, PAM, and NVP-AAM077 bind (Zhu et al., 2016). In the current and previous crystallographic studies, such disruption in the subunit interface did not occur. There are several potential reasons for this different outcome. First, our current study on NVP-AAM077 was conducted in the presence of the co-agonist glycine bound to the GluN1 LBD. Second, our study is conducted in the absence of ATD or TMD, thus, the GluN1-GluN2A LBD is unaffected by conformational movements of these other domains (Romero-Hernandez et al., 2016; Tajima et al., 2016). Third, crystal contacts may be restricting the spatial freedom to potentially disrupt the subunit interaction. Last, the effect of antagonist binding on the overall protein conformation may be different between the GluN1-GluN2A and GluN1-GluN2B NMDA receptors. Nevertheless, our high-resolution structure, along with our electrophysiological assays, clearly indicated that the NVP-AAM077 binding occurs partially at the GluN1-GluN2A subunit interface. Our structural observation indicates that the inhibitory effect of NVP-AAM077 is mostly occurring via opening of the GluN2A

16

LBD bi-lobe as observed in the structural studies of the GluN1-GluN2A LBD complexed to D-AP5 and PPDA (Jespersen et al., 2014). Opening of the GluN2A LBD bi-lobe likely relieves the tension in the LBD-TMD linker (Kazi et al., 2014), thereby preventing channel opening by interfering with a transduction of the physical force from the LBDs to the TMD.

NVP-AAM077 was originally pursued with enthusiasm due to its reported specificity towards the GluN2A-containing NMDA receptors. The extensive study to characterize the NVP-AAM077 pharmacology later showed that the degree of specificity is minimal (Frizelle et al., 2006). Our structural study shows that there is no apparent structural element that qualifies NVP-AAM077 as a GluN2A-specific antagonist as residues from Site-I and Site-III are completely conserved. We expect Site-III in the GluN1-GluN2B subunit interface to be almost identical to the GluN1-GluN2A subunit interface because the subunit arrangement between the GluN1-GluN2A LBD and the GluN1-GluN2B LBD is almost identical (Karakas and Furukawa, 2014). Thus, our study supports little or no subtype-specificity of NVP-AAM077. Nevertheless, the new antagonist binding mode highlighted by the newly observed Site-III provides an opportunity to pursue novel compound designs.

Acknowledgements

crystallography. The structural coordinates related to this work have been deposited to

the Protein Data Bank with the entry code 5U8C.

Authorship Contributions

Participated in research design: Romero-Hernandez, A. and Furukawa, H

Conducted experiments: Romero-Hernandez, A. and Furukawa, H

Performed data analysis: Romero-Hernandez, A. and Furukawa, H

Wrote or contributed to the writing of the manuscript: Romero-Hernandez, A. and
Furukawa, H

References

Adams, P.D., Grosse-Kunstleve, R.W., Hung, L.W., Ioerger, T.R., McCoy, A.J., Moriarty, N.W., Read, R.J., Sacchettini, J.C., Sauter, N.K., and Terwilliger, T.C. (2002). PHENIX: building new software for automated crystallographic structure determination. Acta Crystallogr D Biol Crystallogr *58*, 1948-1954.

Auberson, Y.P., Allgeier, H., Bischoff, S., Lingenhoehl, K., Moretti, R., and Schmutz, M. (2002). 5-Phosphonomethylquinoxalinediones as competitive NMDA receptor antagonists with a preference for the human 1A/2A, rather than 1A/2B receptor composition. Bioorganic & medicinal chemistry letters *12*, 1099-1102.

Auffinger, P., Hays, F.A., Westhof, E., and Ho, P.S. (2004). Halogen bonds in biological molecules. Proc Natl Acad Sci U S A *101*, 16789-16794.

Emsley, P., and Cowtan, K. (2004). Coot: model-building tools for molecular graphics. Acta Crystallogr D Biol Crystallogr *60*, 2126-2132.

Evans, R.H., Francis, A.A., Jones, A.W., Smith, D.A., and Watkins, J.C. (1982). The effects of a series of omega-phosphonic alpha-carboxylic amino acids on electrically evoked and excitant amino acid-induced responses in isolated spinal cord preparations. Br J Pharmacol *75*, 65-75.

Feng, B., Tse, H.W., Skifter, D.A., Morley, R., Jane, D.E., and Monaghan, D.T. (2004). Structure-activity analysis of a novel NR2C/NR2D-preferring NMDA receptor antagonist: 1-(phenanthrene-2-carbonyl) piperazine-2,3-dicarboxylic acid. Br J Pharmacol *141*, 508-516.

Frizelle, P.A., Chen, P.E., and Wyllie, D.J. (2006). Equilibrium constants for (R)-[(S)-1-(4-bromo-phenyl)-ethylamino]-(2,3-dioxo-1,2,3,4-tetrahydroquinoxalin-5   -yl)-methyl]-phosphonic acid (NVP-AAM077) acting at recombinant NR1/NR2A and NR1/NR2B N-methyl-D-aspartate receptors: Implications for studies of synaptic transmission. Mol Pharmacol *70*, 1022-1032.

Furukawa, H., and Gouaux, E. (2003). Mechanisms of activation, inhibition and specificity: crystal structures of the NMDA receptor NR1 ligand-binding core. Embo J *22*, 2873-2885.

Furukawa, H., Singh, S.K., Mancusso, R., and Gouaux, E. (2005). Subunit arrangement and function in NMDA receptors. Nature *438*, 185-192.

Gielen, M., Siegler Retchless, B., Mony, L., Johnson, J.W., and Paoletti, P. (2009). Mechanism of differential control of NMDA receptor activity by NR2 subunits. Nature *459*, 703-707.

Hackos, D.H., Lupardus, P.J., Grand, T., Chen, Y., Wang, T.M., Reynen, P., Gustafson, A., Wallweber, H.J., Volgraf, M., Sellers, B.D.*, et al.* (2016). Positive Allosteric

Modulators of GluN2A-Containing NMDARs with Distinct Modes of Action and Impacts on Circuit Function. Neuron *89*, 983-999.

Jespersen, A., Tajima, N., Fernandez-Cuervo, G., Garnier-Amblard, E.C., and Furukawa, H. (2014). Structural insights into competitive antagonism in NMDA receptors. Neuron *81*, 366-378.

Jin, R., Clark, S., Weeks, A.M., Dudman, J.T., Gouaux, E., and Partin, K.M. (2005). Mechanism of positive allosteric modulators acting on AMPA receptors. J Neurosci *25*, 9027-9036.

Karakas, E., and Furukawa, H. (2014). Crystal structure of a heterotetrameric NMDA receptor ion channel. Science *344*, 992-997.

Karakas, E., Regan, M.C., and Furukawa, H. (2015). Emerging structural insights into the function of ionotropic glutamate receptors. Trends Biochem Sci *40*, 328-337.

Karakas, E., Simorowski, N., and Furukawa, H. (2011). Subunit arrangement and phenylethanolamine binding in GluN1/GluN2B NMDA receptors. Nature *475*, 249-253.

Kazi, R., Dai, J., Sweeney, C., Zhou, H.X., and Wollmuth, L.P. (2014). Mechanical coupling maintains the fidelity of NMDA receptor-mediated currents. Nat Neurosci *17*, 914-922.

Lee, C.H., Lu, W., Michel, J.C., Goehring, A., Du, J., Song, X., and Gouaux, E. (2014). NMDA receptor structures reveal subunit arrangement and pore architecture. Nature *511*, 191-197.

McCoy, A.J., Grosse-Kunstleve, R.W., Adams, P.D., Winn, M.D., Storoni, L.C., and Read, R.J. (2007). Phaser crystallographic software. J Appl Crystallogr *40*, 658-674.

McLennan, H., and Lodge, D. (1979). The antagonism of amino acid-induced excitation of spinal neurons. . Brain Res *169*, 83-90.

Otwinowski, Z., and Minor, W. (1997). Processing of X-ray Diffraction Data Collected in Oscillation Mode. Methods in Enzymology *276*, 307-326.

Regan, M.C., Romero-Hernandez, A., and Furukawa, H. (2015). A structural biology perspective on NMDA receptor pharmacology and function. Curr Opin Struct Biol *33*, 68-75.

Romero-Hernandez, A., Simorowski, N., Karakas, E., and Furukawa, H. (2016). Molecular Basis for Subtype Specificity and High-Affinity Zinc Inhibition in the GluN1-GluN2A NMDA Receptor Amino-Terminal Domain. Neuron.

Sirimulla, S., Bailey, J.B., Vegesna, R., and Narayan, M. (2013). Halogen interactions in protein-ligand complexes: implications of halogen bonding for rational drug design. J Chem Inf Model *53*, 2781-2791.

Stern-Bach, Y., Russo, S., Neuman, M., and Rosenmund, C. (1998). A point mutation in the glutamate binding site blocks desensitization of AMPA receptors. Neuron *21*, 907-918.

Sun, Y., Olson, R., Horning, M., Armstrong, N., Mayer, M., and Gouaux, E. (2002). Mechanism of glutamate receptor desensitization. Nature *417*, 245-253.

Tajima, N., Karakas, E., Grant, T., Simorowski, N., Diaz-Avalos, R., Grigorieff, N., and Furukawa, H. (2016). Activation of NMDA receptors and the mechanism of inhibition by ifenprodil. Nature.

Traynelis, S.F., Wollmuth, L.P., McBain, C.J., Menniti, F.S., Vance, K.M., Ogden, K.K., Hansen, K.B., Yuan, H., Myers, S.J., and Dingledine, R. (2010). Glutamate receptor ion channels: structure, regulation, and function. Pharmacol Rev *62*, 405-496.

Weston, M.C., Schuck, P., Ghosal, A., Rosenmund, C., and Mayer, M.L. (2006). Conformational restriction blocks glutamate receptor desensitization. Nat Struct Mol Biol *13*, 1120-1127.

Williams, K. (1993). Ifenprodil discriminates subtypes of the N-methyl-D-aspartate receptor: selectivity and mechanisms at recombinant heteromeric receptors. Mol Pharmacol *44*, 851-859.

Williams, K. (1997). Interactions of polyamines with ion channels. Biochem J *325 (Pt 2)*, 289-297.

Yi, F., Mou, T.C., Dorsett, K.N., Volkmann, R.A., Menniti, F.S., Sprang, S.R., and Hansen, K.B. (2016). Structural Basis for Negative Allosteric Modulation of GluN2A-Containing NMDA Receptors. Neuron *91*, 1316-1329.

Yuan, H., Hansen, K.B., Vance, K.M., Ogden, K.K., and Traynelis, S.F. (2009). Control of NMDA receptor function by the NR2 subunit amino-terminal domain. The Journal of neuroscience *29*, 12045-12058.

Zhu, S., Stein, R.A., Yoshioka, C., Lee, C.H., Goehring, A., McHaourab, H.S., and Gouaux, E. (2016). Mechanism of NMDA Receptor Inhibition and Activation. Cell *165*, 704-714.

Footnote:

b)

c) Reprint requests to: Hiro Furukawa. Cold Spring Harbor Laboratory. One Bungtown Rd., Cold Spring Harbor, NY 11724, U.S.A. Email: furukawa@cshl.edu

Legends for Figures

Fig. 1. Ligands and domain organization of NMDA receptors. (A) Chemical structures of the agonist glutamate, and competitive antagonists, D-(-)-2-Amino-5-phosphonopentanoic acid (D-AP5), (2S*,3R*)-1-(Phenanthren-2-carbonyl)piperazine-2,3-dicarboxylic acid (PPDA), and (1S)-1-(4-Bromophenyl)ethyl]amino](1,2,3,4-tetrahydro-2,3-dioxo-5-quinoxalinyl)methyl] phosphonic acid (NVP-AAM077). **(B)** Domain organization of NMDA receptor subunits, which are composed of an amino terminal domain (ATD), an agonist-binding domain (LBD), a transmembrane domain (TMD), and a carboxy-terminal domain (CTD). The LBD is isolated by tethering the two peptides separated by the M1 and M3 TMD helices by a Gly-Thr dipeptide linker (dots).

Fig. 2. Crystal structure of NVP-AAM077-GluN1-GluN2A LBD. (A) The crystal structure of the GluN1-GluN2A LBD complexed to glycine (light grey spheres) and NVP-AAM077 (yellow spheres) to GluN1 and GluN2A, respectively, viewed from the side. Spheres with asterisks are the Cαs of the Gly-Thr linker. Cysteine residues forming disulfide bonds are shown as sticks. The LBDs have a clamshell-like architecture composed of two bi-lobe domains, D1 (green in GluN1 and purple in GluN2A) and D2 (orange in GluN1 and magenta in GluN2A). **(B)** The same structure viewed from the 'top' of the N-termini. The bromophenyl group of NVP-AAM077 extends towards Helix I of the GluN1 subunit (dotted oval).

Fig. 3. Comparison of NVP-AAM077-GluN1-GluN2A LBD with glu-GluN1-GluN2A LBD. (A) Comparison of the GluN1-GluN2A heterodimers by superposition of the D1 of the GluN2A LBDs bound to glutamate (PDB code: 4NF8) and NVP-AAM077. The color code for the NVP-AAM077-GluN1-GluN2A LBD is the same as in Fig. 1. The structure of the glutamate-bound GluN1-GluN2A LBD (glu-GluN1-GluN2A LBD) is in grey. **(B)** The same superposed structures viewed from a different angle. Only GluN2A LBD is shown here for clarity. The rotational angle to superpose Cαs of D2 is calculated to be 17° around the pivotal axis shown as a black rod, which indicates that the NVP-AAM077-bound GluN2A LBD is 17° more 'open' than the glutamate-bound GluN2A LBD. No significant change was observed in GluN1 LBDs between the two structures. **(C)** Schematic illustration to show that the domain 'opening' in GluN2A reduces the distance between the LBD-TMD linkers of GluN1 and GluN2A subunits, thereby reducing the 'tension' necessary for channel gating.

Fig. 4. Binding site of NVP-AAM077. (A) Stereoview of the NVP-AAM077 binding site. The binding of NVP-AAM077 (yellow sticks) is mediated by a number of polar interactions and a halogen interaction (black dashed lines). The carboxyl side chain of GluN1-Glu781 (green sticks) interacts with the bromine atom in the bromophenyl group of NVP-AAM077 via a halogen bond. **(B)** The *Fo-Fc* omit map of NVP-AAM077 contoured at 3σ illustrates clear density for every chemical feature of the compound. **(C)** Schematic illustration of the NVP-AAM077 binding site. The phosphono group and the bromophenyl group occupy Site-I and Site-III, respectively, while no chemical group binds to Site-II.

24

Fig. 5. NVP-AAM077 forms halogen bond with GluN1-Glu781. (A and B) The *2Fo-Fc* map contoured at 1.5σ shows ordered electron density for the residue GluN1-Glu781, a water molecule W3, and NVP-AAM077. Electron density for other residues and water molecules is omitted for clarity. **(C)** The GluN1-GluN2A subunit interface in the glutamate-bound GluN1-GluN2A LBD structure (PDB code: 4NF8). **(D)** The same interface in the NVP-AAM077-bound GluN1-GluN2A LBD structure. The placement of the bromophenyl group displaces three water molecules (W4-6) that are forming inter-subunit interactions between GluN1-Glu781 and GluN2A-Ser689 or GluN2A-Thr690. The distance between the carboxyl oxygen in GluN1-Glu781 and the bromine atom in the bromophenyl group is 3.5 Å in this structure.

Fig. 6. Validation of NVP-AAM077-GluN1 interaction (A) Mutational analysis of the mutant channels containing GluN1-Glu781Ala or GluN1-Glu781Asp and the wildtype GluN2A by TEVC. Dose-response of glutamate was measured in the presence of 100 µM glycine. **(B)** Inhibition of the NMDA receptor currents by various concentrations of NVP-AAM007 in the presence of 100 µM glycine and 5 µM glutamate. **(C)** K_i values were calculated with the Cheng-Prusoff equation as described in the 'Materials and Methods' section and compared with that of the wildtype channel. Data points were acquired from independent recording using six different *Xenopus* oocytes. Error bars represent SD.

Table 1. Data collection and Refinement Statistics

	GluN1-GluN2A ABD NVP-AAM077
Data collection	
Resolution (Å)	50-1.6 (1.66-1.60)
Space Group	$P2_12_12_1$
Unit cell dimensions	
a (Å)	59.550
b (Å)	84.227
c (Å)	121.218
Completeness (%)	89.5 (55.3)
R_{merge}	0.077 (0.623)
Redundancy	4.3 (1.6)
$I//\sigma$	17.84 (1.23)
Refinement	
No. of unique reflections	72823
R_{work}/R_{free}	0.20/0.22
No. atoms	
Protein	4300
Compound	27
Water	253
Glycerol	0
B factors	
Protein	22.34
Compound	16.41
Water	25.64
Glycerol	--
RMSD	
Bond lengths (Å)	0.008
Bond angles (°)	1.101

[a] Values in parentheses are for the highest-resolution shell.

Table 2. Potency of NVP-AAM077

	Glutamate	NVP-AAM077	NVP-AAM077	NVP-AAM077
	EC_{50} µM	IC_{50} nM	K_i nM	K_i - fold increase
GluN1-GluN2A WT	3.81 ± 0.89	68..40 ± 3.79	29.58 ± 0.24	-
GluN1 E781D	8.55 ± 1.54	636.9 ± 79.35	401.93 ± 0.21	13.58 ± 0.008
GluN1 E781A	20.85 ± 3.39	344.47 ± 42.94	277.84 ± 0.20	9.39 ± 0.008

IC_{50} values were calculated in the presence of 5 µM glutamate and 100 µM glycine for all of the mutants.
K_i values were calculated by the Cheng- Prusoff equation: $K_i = \dfrac{IC_{50}}{1+\frac{[L-glutamate]}{EC_{50}}}$

EC_{50} and IC_{50} ± s.d. represents values from three and six different oocytes per experiment, respectively.

± s.d. for K_i and K_i fold was calculated with the Error Propagation formula as follows:

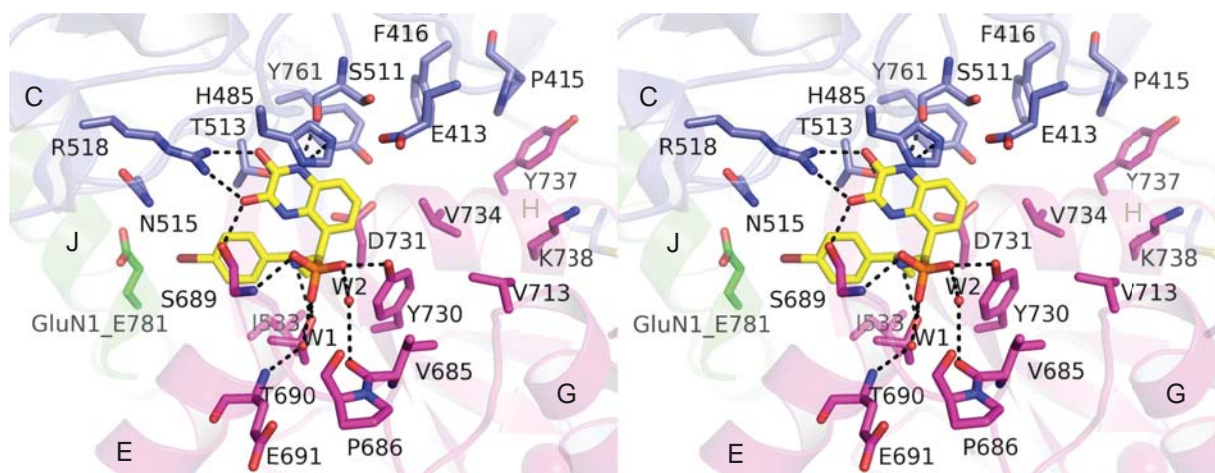$$\frac{\delta Q}{Q} = \sqrt{\left(\frac{\delta a}{a}\right)^2 + \cdots + \left(\frac{\delta z}{z}\right)^2}$$
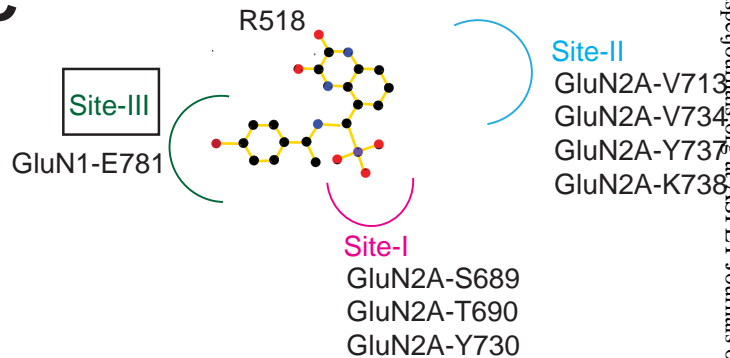
Fig. 1

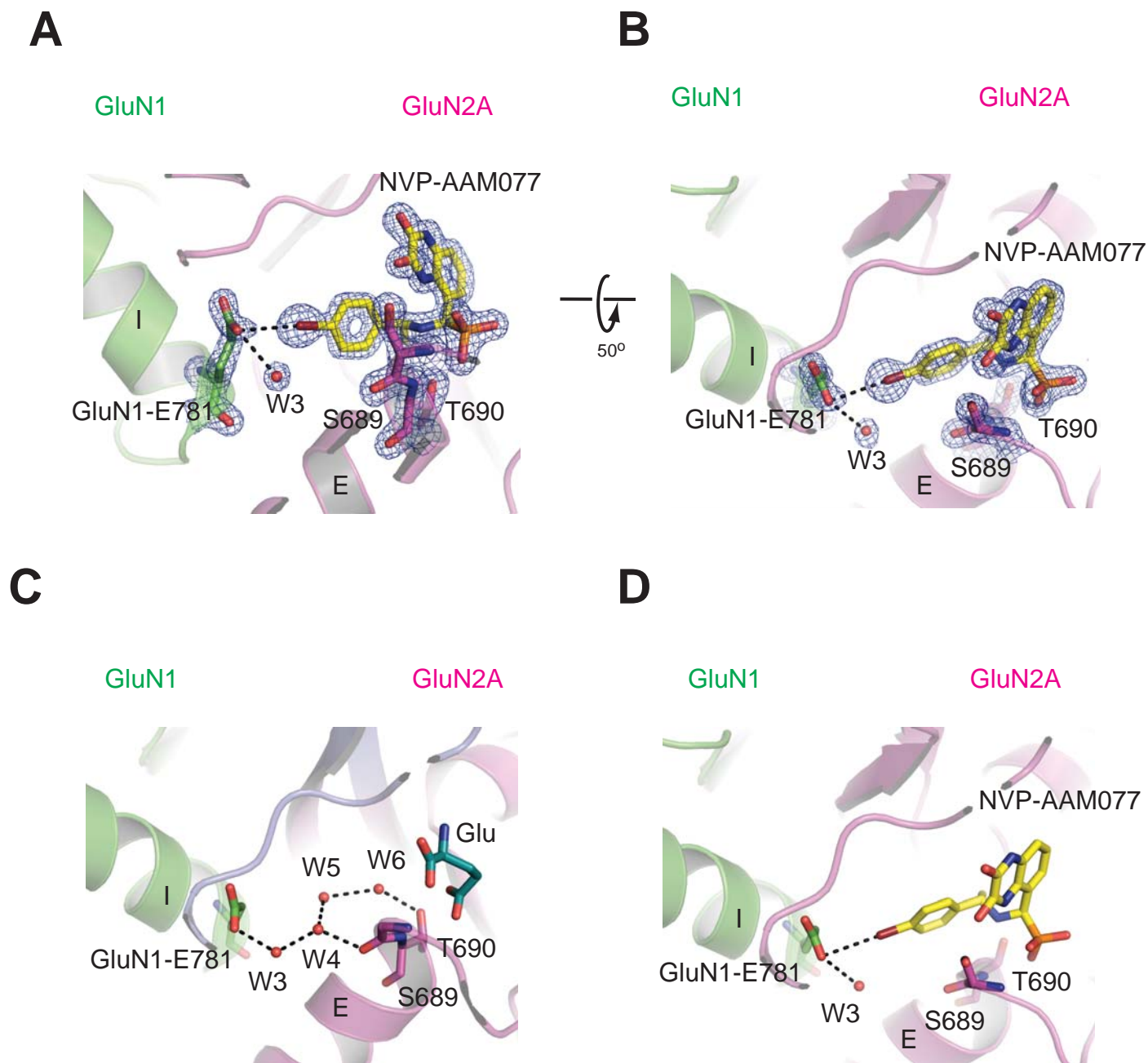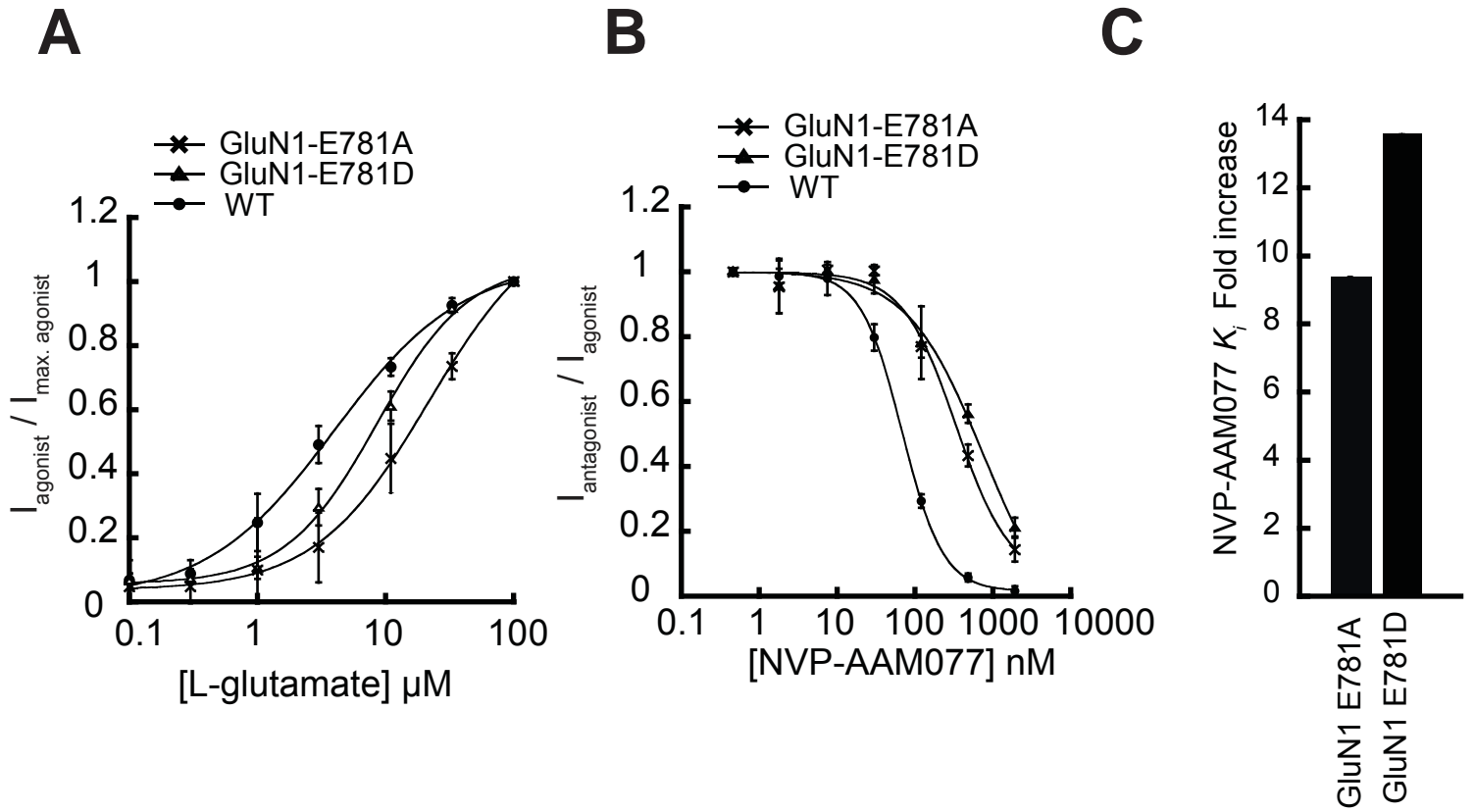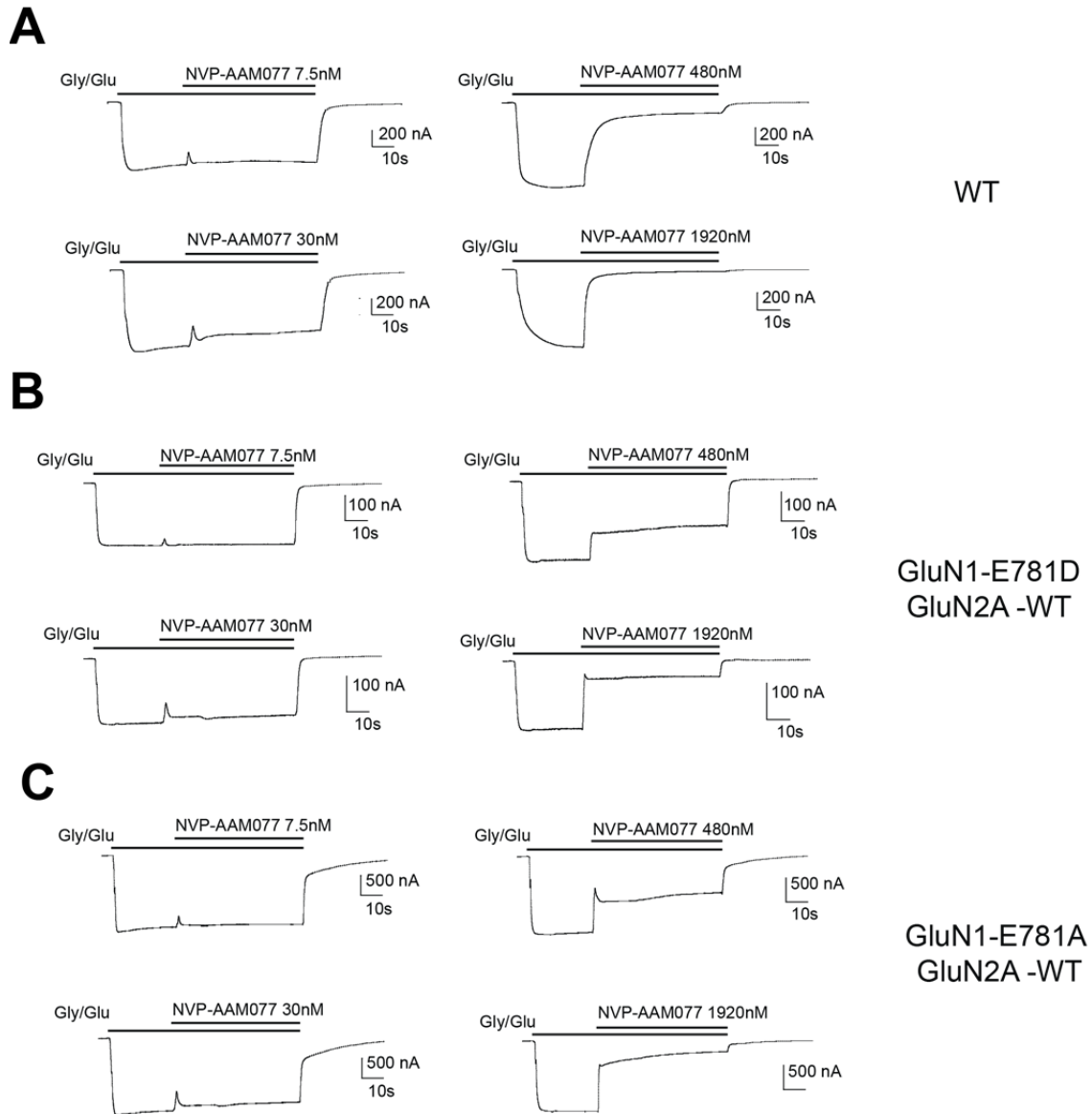GluN1 (gly) - GluN2A (NVP-AAM0077)
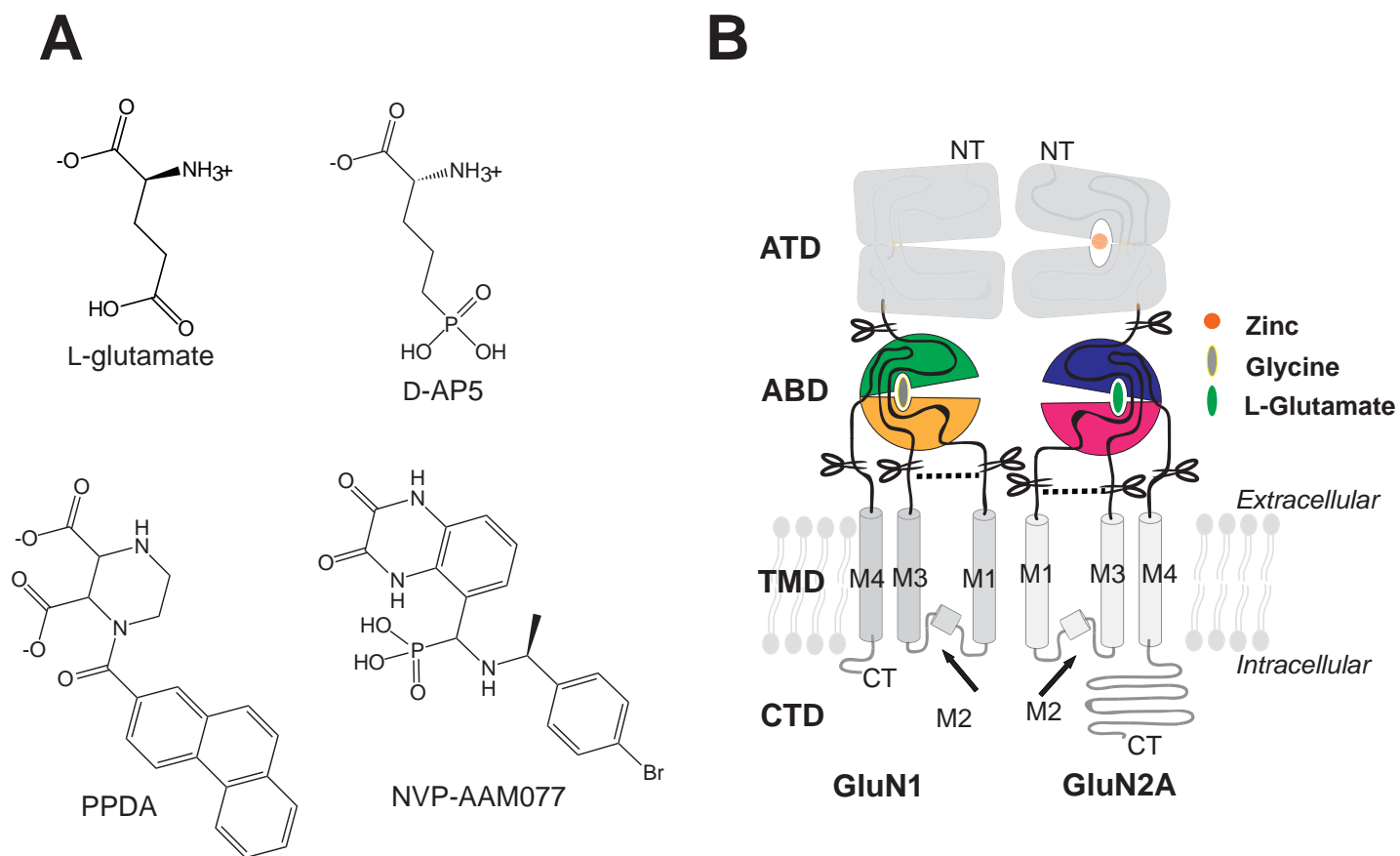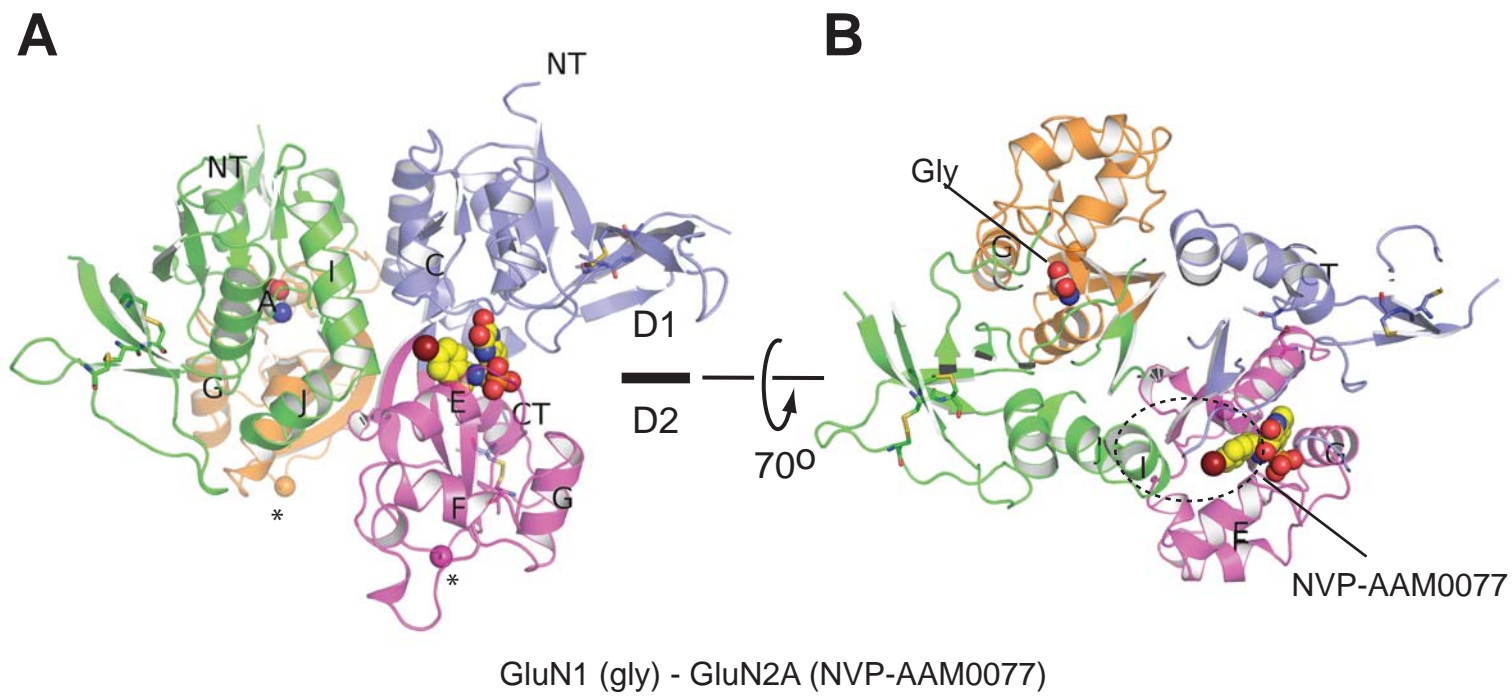
Fig. 2
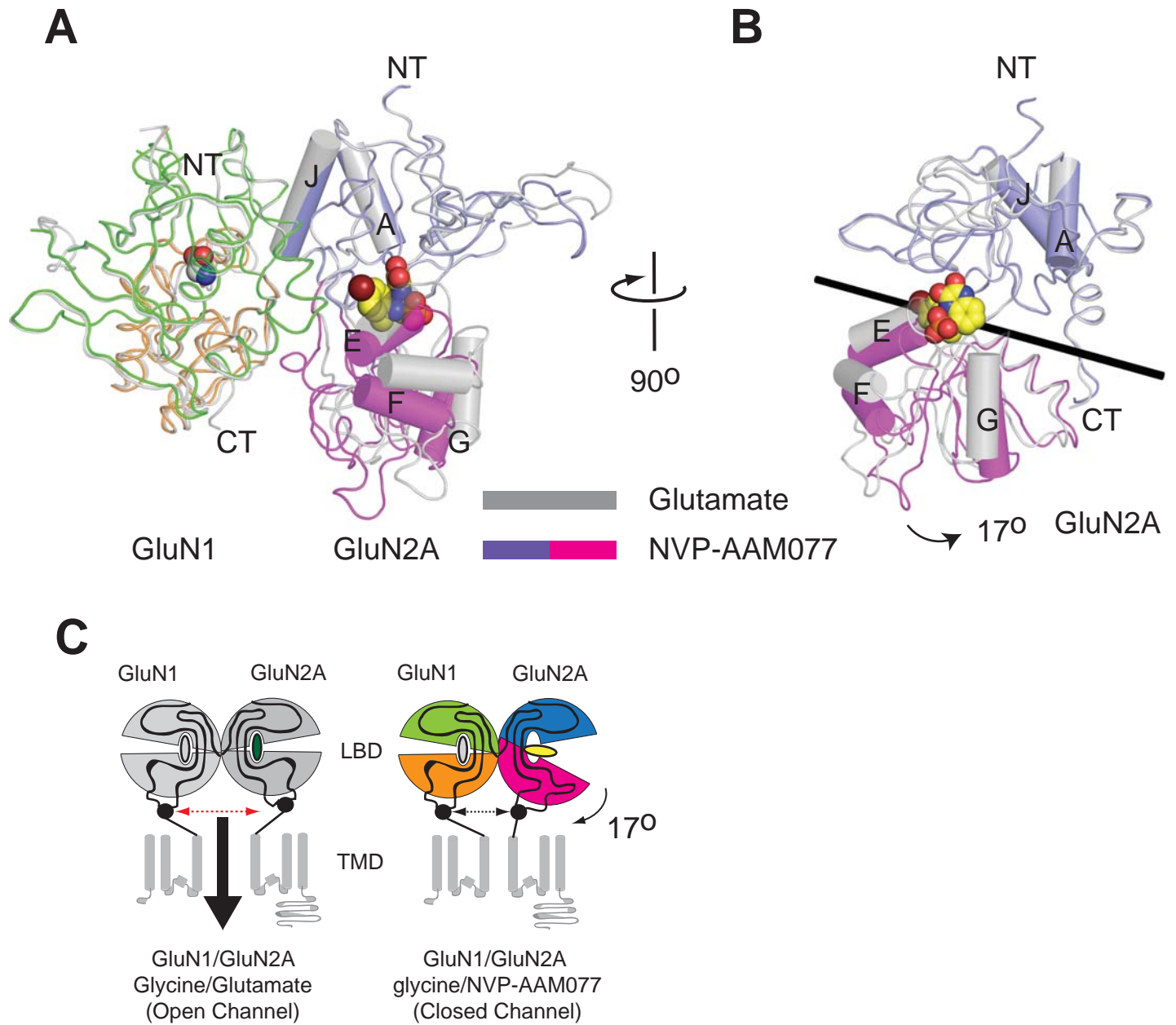
Fig. 3
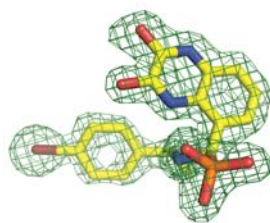
Fig. 4

Fig. 5

Fig. 6

Novel mode of antagonist binding in NMDA receptors revealed by the crystal structure of the GluN1-GluN2A ligand-binding domain complexed to NVP-AAM077
Annabel Romero-Hernandez and Hiro Furukawa
Molecular Pharmacology

Supplemental Fig. 1.

Monitoring inhibition by NVP-AAM007 using TEVC. Representative recordings of GluN1-1a WT-GluN2A WT (A), GluN1-1a-E781D-GluN2A WT (B), and GluN1-1a-E781A-GluN2A WT (C). All recordings were performed at various concentrations of NVP-AAM007 in the presence of 100 µM glycine and 5 µM glutamate. Show here are recordings done in the presence of NVP-AAM007 at 7.5 nM, 30 nM, 480 nM, and 1920 nM.